Ubiquitin-binding domain in ABIN1 is critical for regulating cell death and inflammation during development

Haibing Zhang (hbzhang@sibs.ac.cn)
University of Chinese Academy of Sciences, Chinese Academy of Sciences https://orcid.org/0000-0002-8814-7378

Ming Li
Institute for Nutritional Sciences, Shanghai Institutes for Biological Sciences

Yongbo Liu
Institute for Nutritional Sciences, Shanghai Institutes for Biological Sciences

Chengxian Xu
Institute for Nutritional Sciences, Shanghai Institutes for Biological Sciences

Qun Zhao
University of Chinese Academy of Sciences, Chinese Academy of Sciences

Jianling Liu
University of Chinese Academy of Sciences, Chinese Academy of Sciences

Mingyan Xing
University of Chinese Academy of Sciences, Chinese Academy of Sciences

Xiaoming Li
Institute for Nutritional Sciences, Shanghai Institutes for Biological Sciences

Hai-Wei Zhang
Shanghai Institutes for Biological Sciences, Chinese Academy of Sciences, University of Chinese Academy of Sciences

Xiaoxia Wu
Institute for Nutritional Sciences, Shanghai Institutes for Biological Sciences

Lingxia Wang
University of Chinese Academy of Sciences, Chinese Academy of Sciences

Yangjing Ou
University of Chinese Academy of Sciences, Chinese Academy of Sciences

Xuanhui Wu
Shanghai Institute of Nutrition and Health, University of Chinese Academy of Sciences, Chinese Academy of Sciences

Xiaoming Zhao
University of Chinese Academy of Sciences, Chinese Academy of Sciences

Han Liu
University of Chinese Academy of Sciences, Chinese Academy of Sciences
Fang Li
University of Chinese Academy of Sciences, Chinese Academy of Sciences
Jin Bao Li
University of Chinese Academy of Sciences, Chinese Academy of Sciences https://orcid.org/0000-0001-5582-5737
Wuwei Rong
Ruijin Hospital/Shanghai Jiaotong University
Jiangshan Deng
Shanghai Jiao Tong University Affiliated Sixth People's Hospital
Xiuzhe Wang
Shanghai Jiao Tong University Affiliated Sixth People's Hospital
Zhichao Wang
Zhongshan Hospital; Key Laboratory of Carcinogenesis and Cancer Invasion, Ministry of Education, Fudan University
Yuwu Zhao
Shanghai Jiao Tong University Affiliated Sixth People's Hospital
Ankang Lv
Ruijin Hospital/Shanghai Jiaotong University
Qingfeng Li
Shanghai Ninth People's Hospital□Shanghai Jiao Tong University School of Medicine

---

Article

Keywords: ABIN1, cell death, immune disease

Posted Date: July 26th, 2021

DOI: https://doi.org/10.21203/rs.3.rs-712049/v1

Abstract

ABIN1 is a polyubiquitin-binding protein known to regulate NF-κB activation and cell death signaling. Mutations in *Abin1* can cause severe immune diseases in human, such as psoriasis, systemic lupus erythematosus, and systemic sclerosis. Here, we generated mice that disrupted the ubiquitin-binding domain of ABIN1 (*Abin1*$^{UBD/UBD}$) died during later embryogenesis owing to TNFR1-mediated cell death, similar to *Abin1*$^{-/-}$ mice. *Abin1*$^{UBD/UBD}$ cells were rendered sensitive to TNF-α-induced apoptosis and necroptosis as the inhibition of ABIN1^{UBD} and A20 recruitment to the TNF-RSC complex leads to attenuated RIPK1 deubiquitination. Accordingly, the embryonic lethality of *Abin1*$^{UBD/UBD}$ mice was rescued via crossing with RIPK1 kinase-dead mice (*Ripk1*$^{K45A/K45A}$) or the co-deletion of *Ripk3* and one allele of *Fadd*, but not by the loss of *Ripk3* or *Mlkl* alone. Unexpectedly, *Abin1*$^{UBD/UBD}$ mice with the co-deletion of *Ripk3* and both *Fadd* alleles died at E14.5. This death was caused by spontaneous RIPK1 ubiquitination-dependent multiple inflammatory cytokines over production and could be rescued by the co-deletion of *Ripk1* or *Tnfr1* combined with *Ifnar*. Collectively, these data demonstrate the importance of the ABIN1 UBD domain, which mediates the ABIN1-A20 axis, at limiting RIPK1 activation-dependent cell death during embryonic development. Furthermore, our findings reveal a previously unappreciated ubiquitin pathway that regulates cleavage of ubiquitinated RIPK1 by FADD/Casp8 to suppress spontaneous IKKε/TBK1 activation.

Introduction

ABIN1, also referred to as TNF-α-induced protein 3-interacting protein 1, is a polyubiquitin-binding protein that has been implicated in the regulation of cell death, inflammation, and immunity, and has been linked to multiple human inflammatory diseases, including psoriasis, psoriatic arthritis, SLE, and systemic sclerosis[1, 2, 3, 4, 5, 6]. ABIN1 is a member of the ABIN homology domain (AHD) protein family that mediates A20 binding and polyubiquitin binding. ABIN1 contains a ubiquitin-binding domain (UBD) that binds to polyubiquitin and polyubiquitinated proteins and a NEMO binding domain (NBD) at the C-terminus, both of which have been demonstrated to participate in the inhibition of NF-κB activation[7, 8]. In particular, the ABIN1 inhibitory functions on NF-κB activation and antiviral signaling have been reported to rely on its polyubiquitin chain binding ability mediated by the UBD domain, as point mutations in this domain could abolish its inhibitory functions[7, 8]. Moreover, ABIN1 knock-in mice harboring a mutation within the UBD domain (D485N, homologous to human D472N) were viable and developed severe inflammation in multiple organs after 5-6 months[9], in sharp contrast to the embryonic lethality observed in *Abin1* knockout mice[10]. Such findings suggest that the D485N mediated disruption of the polyubiquitin binding ability of ABIN1 is not essential for embryonic development. The caveat here is that the D485N mutation might not completely disrupt the polyubiquitin binding ability of ABIN1; thus, the physiological role of the UBD domain of ABIN1 remains unclear.

Previous studies have shown that ABIN1 binds linear ubiquitin chains on NEMO and A20 to promote the deubiquitination and termination of NF-κB signaling[7, 9, 10, 11, 12, 13, 14]. In addition, upon TNF-α stimulation,

ABIN1 is recruited to the TNFR1 signaling complex (TNF-RSC) and subsequently recruits A20, which mediates the deubiquitination of RIP kinase 1 (RIPK1) to suppress necroptosis[15, 16]. Furthermore, the embryonic lethality of *Abin1*-deficient mice was rescued via crossing with *Ripk3* knockout or RIPK1 kinase inactive mutant mice to block necroptosis [15]. Such findings imply that ABIN1 plays a critical role in suppressing RIPK3-mediated necroptosis during development. However, the physiological contribution of the ABIN1 UBD domain in this process remains unclear.

Besides its role in regulating cell death and NF-kB signaling, ABIN1 has been shown to modulate antiviral signaling pathways by cooperating with A20[8, 17, 18, 19]. Previous studies have revealed that ABIN1 can recruit TAX1BP1 and A20 to assemble the A20 regulatory complex by sensing Lys-63-linked polyubiquitin chains via its UBD, and subsequently inhibit type I IFNs production mediated antiviral signaling by disrupting the interactions between TRAF2 and TBK1/IKKε to attenuate TBK1/IKKε polyubiquitination[8]. Furthermore, ABIN1 heterozygous mouse has enhanced antiviral response *in vivo* by potentially promoting the expression of key viral pattern recognition molecules, which is partially mediated by RIPK1 kinase activity[17]. These studies indicate that ABIN1 plays critical roles in regulating antiviral responses. However, the mechanisms by which ABIN1 regulates the physiological antiviral signaling pathway remains unknown.

In this study, we generated knock-in mice with a disrupted ABIN1 polyubiquitin binding domain (*Abin1*$^{UBD/UBD}$). *Abin1*$^{UBD/UBD}$ mice resembled *Abin1*$^{-/-}$ mice and died at a later embryogenesis stage owing to cell death mediated by TNFR1 and the kinase activity of RIPK1. Such finding indicates that the function of the UBD domain of ABIN1 is indispensable for embryonic development. Furthermore, we found that the embryonic lethality of *Abin1*$^{UBD/UBD}$ mice was rescued by the co-deletion of *Ripk3* and one allele *Fadd*, while the deletion of *Ripk3* or *Mlkl* alone had no effect. Surprisingly, the ablation of *Ripk3* and two alleles of *Fadd* from *Abin1*$^{UBD/UBD}$ mice resulted in embryonic lethality at E14.5, owing to spontaneous RIPK1 ubiquitination-dependent multiple inflammatory cytokines over production. Remarkably, the lethality of *Abin1*$^{UBD/UBD}$*Fadd*$^{-/-}$*Ripk3*$^{-/-}$ mice can be rescued by the co-deletion of *Tnfr1* and *Ifnar*. Thus, these results demonstrate the significant contributions of the ABIN UBD domain in regulating cell death and IKKε/TBK1 pathway mediated the production of multiple inflammatory cytokines during development.

Results

The UBD domain of ABIN1 is required for the prevention of TNFR1 signaling-induced embryonic lethality

Although ABIN1, a ubiquitin binding protein, is required to restrict NF-κB activation and regulate cell death upon stimulation with TNF-α and TLRs[9, 10, 15], the specific contributions of the UBD domain of ABIN1 *in vivo* remain unknown. To determine the physiological role of the ABIN1 UBD domain, we generated *Abin1* mutant mice with exon 13 deletion at the transcriptional level using the CRISPR/Cas9 technology (hereafter termed as Abin1$^{UBD/UBD}$ mice) (**Supplementary Fig.1a**), which caused a deletion of the aa452-

478 in the UBD domain (**Supplementary Fig.1 b-d**). In contrast to the viable *Abin1*$^{D485N/D485N}$ mice expressing ABIN1 with a D485N point mutation in the UBD domain, no *Abin1*$^{UBD/UBD}$ mice survived to the weaning age following heterozygous intercrossing (**Fig.1 a**). Examination of pups obtained from timed mating revealed that *Abin1*$^{UBD/UBD}$ mice were alive at E16.5, but died perinatally (**Fig.1 b**), similar to *Abin1*$^{-/-}$ mice. Histological analysis of embryos at E16.5 revealed a reduced number of cells in fetal liver, an increase in the apoptotic marker, cleaved Casp3, and increased TUNEL^{+} cells in *Abin1*$^{UBD/UBD}$ embryos (**Fig.1 c**). Furthermore, immunoblot analysis revealed the presence of cleaved PARP and Casp3, markers of apoptosis, in the NP-40 soluble fraction of the *Abin1*$^{UBD/UBD}$ embryo lysate. The necroptosis components containing RIPK1, RIPK3, MLKL, and phosphorylated MLKL were also aggregated in the soluble fraction of 6 M urea (**Fig.1 d**). These findings demonstrate that both apoptosis and necroptosis occurred simultaneously in the *Abin1*$^{UBD/UBD}$ embryos.

TNF-α signaling has been reported to be required for perinatal death induced by *Abin1* knockout[10, 20]. To determine whether the perinatal lethality of *Abin1*$^{UBD/UBD}$ mice is also mediated by TNFR1 signaling, we crossed *Abin1*$^{UBD/UBD}$ mice with *Tnfr1*$^{-/-}$ animals. Knocking out *Tnfr1* could overcome perinatal lethality in *Abin1*$^{UBD/UBD}$ mice (**Fig.1 e-f**), confirming that TNFR1 signaling is also essential for perinatal death in *Abin1*$^{UBD/UBD}$ mice. Therefore, in contrast to *Abin1*$^{D485N/D485N}$ mice harboring a D485N point mutation in the UBD domain of ABIN1, which is fertile, the perinatal death of *Abin1*$^{UBD/UBD}$ mice was found to be caused by the activation of TNFR1 signaling, demonstrating the essential role of the ABIN1 UBD domain in the regulation of embryonic development.

ABIN1 UBD domain is essential for restricting RIPK1 activation-mediated cell death

To study the putative contributions of the ABIN1 UBD domain to different signaling pathways involving ABIN1, we generated *Abin1*$^{UBD/UBD}$ mouse embryonic fibroblasts (MEFs) and treated them with TNF/Smac (TS) or TNF/CHX (TC) to induce apoptosis and TNF/Smac/zVAD (TSZ) or TNF/CHX/zVAD (TCZ) to induce necroptosis. *Abin1*$^{UBD/UBD}$ MEFs were found to be more sensitive to TS- or TC-induced apoptosis and TSZ- or TCZ-induced necroptosis compared to WT MEFs (**Supplementary Fig.2 a-b**). In contrast, *Abin1*$^{UBD/UBD}$ MEFs cells displayed similar sensitivity to the Staurosporine (STS)-induced endogenous pathway of apoptosis and NF-κB activation stimulated by TNF-α to WT MEFs (**Supplementary Fig.2 c-d**). These results suggest that the UBD domain of ABIN1 is critical for restricting TNF-α-mediated apoptosis and necroptosis, but is not essential for NF-κB activation and the endogenous apoptosis pathway. Nec-1, a kinase inhibitor of RIPK1[21], was also found to strongly inhibit cell death caused by various stimuli, including TNF/Smac, TNF/CHX, TNF/5z7, TNF/TPCA, and those combined with ZVAD in *Abin1*$^{UBD/UBD}$ MEFs (**Supplementary Fig.3 a-f**). Such findings suggest that ABIN1 prevented RIPK1 kinase-mediated cell death through its UBD domain. We characterized the signaling complexes in TNF-α-treated *Abin1*$^{UBD/UBD}$ MEFs. In TNF-α-stimulated *Abin1*$^{UBD/UBD}$ MEFs, the ubiquitination of RIPK1 significantly increased and the level of p-Ser166 RIPK1 was elevated at the late time points (**Fig.2 a**). Furthermore, increased p-Ser166 RIPK1, but not enhanced ubiquitination of RIPK1, was inhibited in the

presence of Nec-1 or the genetic kinase inactive mutant, RIPK1 K45A (**Fig.2 b-c**). Such finding suggests that the ABIN1 UBD domain is required for restricting the ubiquitination of RIPK1, which precedes RIPK1 phosphorylation-dependent activation. We proceeded to determine whether complex II formation and cell death increased in TNF-α-treated *Abin1*$^{UBD/UBD}$ MEFs. The components of TNF-α-induced complex II, including RIPK1, RIPK3, FADD, and MLKL, were found to be significantly elevated in *Abin1*$^{UBD/UBD}$ MEFs compared to those in WT MEFs (**Fig.2 d**), resulting in the sensitization to TNF-α-induced apoptosis and necroptosis (**Fig.2 e-g**). Therefore, the UBD domain of ABIN1 is essential for inhibiting RIPK1 ubiquitination, activation, and complex II formation to prevent apoptosis and necroptosis.

The ABIN1 UBD domain supports the recruitment of A20 to TNF-RSC by recognizing and binding to the ubiquitinated RIPK1

In the absence of RIPK1, ABIN1 could not be recruited into TNF-RSC, resulting in the reduced recruitment of A20 (**Fig.3 a**). To further investigate how ABIN1 regulates RIPK1 ubiquitination and activation-mediated cell death through its UBD domain, we hypothesized that the recruitment of ABIN1^{UBD} and A20 to TNF-RSC could be affected when RIPK1 ubiquitination is abolished. CIAP1/2 is a ubiquitin ligase that catalyzes RIPK1 ubiquitination and can be degraded by BV6 treatment[22, 23]. As expected, MEFs pretreated with BV6 had reduced levels of ubiquitinated RIPK1 and reduced recruitment of ABIN1 and A20 in TNF-RSC (**Fig.3 b**), consistent with the results using Smac pretreatment[15]. These findings suggest that ABIN1 recruitment depends on the RIPK1 ubiquitination status. In RIPK1^{K376R} mutant MEFs, which had defective RIPK1 ubiquitination[24, 25, 26], we observed the same reductions and further confirmed the effect of RIPK1 ubiquitination on the TNF-RSC recruitment of ABIN1 (**Fig.3 c**). Treatment with the RIPK1 kinase inhibitor (Nec-1) or genetic kinase dead mutant of RIPK1 (*Ripk1*$^{K45A/K45A}$) had no effect on the ubiquitination of RIPK1 and the recruitment of ABIN1 and A20 in TNF-RSC (**Fig.3 d-e**). Hence, these results suggest that ABIN1 recruits A20 to TNF-RSC by binding to ubiquitinated RIPK1, which are upstream events of RIPK1 kinase activation. To investigate whether the recruitment efficiency of A20 to TNF-RSC was regulated by the ABIN1 UBD, we compared the TNF-RSC components in *Abin1*$^{UBD/UBD}$ MEFs to those in WT MEFs after the cells were treated with flag-TNF-α. We found that the mutant ABIN1^{UBD} could not be recruited to TNF-RSC, resulting in the reduced recruitment of A20 and phosphorylated A20. However, there was no effect on the recruitment of other TNF-RSC components (including TAK1, TRADD, cIAP1/2, NEMO, and SHARPIN) (**Fig.3 f**). Phosphorylated A20 is the catalytically active form of A20, which hydrolyzes and removes ubiquitin from ubiquitylated RIPK1 in TNF-RSC[13, 14, 27, 28]. Through tandem ubiquitin binding entity (TUBE)-pull down, we found that the levels of K63 ubiquitin chains and linear (M1-linked) ubiquitin chains on RIPK1 significantly increased in TNF-α-stimulated *Abin1*$^{UBD/UBD}$ MEFs compared to those in WT MEFs (**Fig.3 g**). These results indicate that the ABIN UBD domain is essential for ABIN1's function in recruiting A20 to TNF-RSC, thereby inhibiting RIPK1 activation-mediated cell death.

Abin1$^{UBD/UBD}$ mice died from RIPK1 kinase or FADD/RIPK3-dependent apoptosis and necroptosis

Although *Abin1* deficiency promotes RIPK1 kinase activity mediated both apoptosis and necroptosis *in vitro*, the perinatal lethality of *Abin1* deficient mice was rescued by crossing RIPK1 kinase dead mutant mice ($Ripk1^{D138N/D138N}$) or crossing RIPK3 knock-out mice alone[15]. These findings suggest that blocking RIPK3-dependent necroptosis is sufficient to recover perinatal death of *Abin1* deficient mice. As $Abin1^{UBD/UBD}$ mice died perinatally and resembled *Abin1* deficient mice, we used a genetic strategy to unravel the mechanisms whereby ABIN1 regulates RIPK1 activation and cell death through its UBD domain. The genetic inactivation of RIPK1 ($Ripk1^{K45A/K45A}$) prevented the lethality of $Abin1^{UBD/UBD}$ mice (**Fig.4 a-b**). Further, the statistical results of the offspring at weaning aligned with Mendel's genetic law (**Fig.4 a**). Accordingly, $Abin1^{UBD/UBD}Ripk1^{K45A/K45A}$ MEFs were resistant to cell death induced by both apoptotic and necroptotic stimuli (**Fig.4 d-f, Supplementary Fig.3 g-i**). However, the deletion of necroptotic components ($Ripk3^{-/-}$ or $Mlkl^{-/-}$) alone only delayed the lethality of $Abin1^{UBD/UBD}$ mice at approximately 1-2 days (**Supplementary Fig.4 a-e**). Remarkable amounts of cleaved Casp3 and Casp8 were still detected in the liver tissues of $Abin1^{UBD/UBD}Ripk3^{-/-}$ mice (**Supplementary Fig. 4 f**). Immunohistochemical results also confirmed the presence of cleaved Casp3 in the liver tissue of $Abin1^{UBD/UBD}Ripk3^{-/-}$ mice (**Supplementary Fig. 4g**), suggesting that the $Abin1^{UBD/UBD}Ripk3^{-/-}$ mice could die from excessive apoptosis. This notion is supported by the result that the absence of a single allele of *Fadd* rescued $Abin1^{UBD/UBD}Ripk3^{-/-}$ mice from death (**Fig.4 a, c**). Surprisingly, no surviving $Abin1^{UBD/UBD}Fadd^{-/-}Ripk3^{-/-}$ mice were observed in the offspring after birth by interbred of the $Abin1^{UBD/+}Fadd^{+/-}Ripk3^{-/-}$ mice (**Fig.4 a**). *In vitro* cell death analysis revealed that either $Fadd^{+/-}Ripk3^{-/-}$ or $Fadd^{-/-}Ripk3^{-/-}$ inhibited both apoptosis and necroptosis in $Abin1^{UBD/UBD}$ MEFs (**Fig.4 g-i**), suggesting that the embryonic lethality of $Abin1^{UBD/UBD}$ could be caused by RIPK1 kinase-mediated apoptosis and necroptosis. $Abin1^{UBD/UBD}Ripk1^{K45A/K45A}$ and $Abin1^{UBD/UBD}Fadd^{+/-}Ripk3^{-/-}$ mice overcame the perinatal lethality of $Abin1^{UBD/UBD}$ mice; however, they displayed lymphadenopathy and splenomegaly at 8-weeks-old (**Supplementary Fig.5a, 5 g**). Flow analysis revealed that the numbers of B cells, activated T cells, and granulocytes ($Gr\text{-}1^{+}Cd11b^{+}$) were significantly increased in the spleens and lymph nodes of $Abin1^{UBD/UBD}Ripk1^{K45A/K45A}$ and $Abin1^{UBD/UBD}Fadd^{+/-}Ripk3^{-/-}$ mice (**Supplementary Fig.5 a-j**), which was similar to the spontaneous immune system development defects observed in $Abin1^{D485N/D485N}$ mice. These results indicate that the UBD domain of ABIN1 is not only required for inhibiting RIPK1 kinase-mediated cell death, but is also essential for maintaining immune homeostasis.

ABIN1 suppresses the production of multiple cytokines through its UBD domain in the $Fadd^{-/-}Ripk3^{-/-}$ background

As $Fadd^{-/-}Ripk3^{-/-}Abin1^{UBD/UBD}$ mice did not survive after birth, this implies that the ABIN1 UBD domain plays a pivotal role during development in a cell death-independent manner. We carried out a more in-depth evaluation of $Fadd^{-/-}Ripk3^{-/-}Abin1^{UBD/UBD}$ mice. Analysis of the pregnant mice revealed that $Abin1^{UBD/UBD}Fadd^{-/-}Ripk3^{-/-}$ mice appeared abnormal at mid-gestation and no viable embryos appeared after E15.5 days (**Fig. 5 a, Supplementary Fig.6 a-b**), indicating that $Abin1^{UBD/UBD}Fadd^{-/-}Ripk3^{-/-}$ mice died at mid-gestation. As the ABIN1 UBD domain is essential for ABIN1 function in A20 recruitment to TNF-

RSC, we tested whether the loss of A20 combined with the co-deletion of FADD and RIPK3 also leads to early embryonic lethality. We observed that A20 deficient mice died approximately two weeks after birth, consistent with previous reports[29]. However, although mice with inactivated RIPK1 kinase mutations (*Ripk1*$^{K45A/K45A}$) prolonged the survival of *A20*$^{-/-}$ mice[30], the *A20*$^{-/-}$*Fadd*$^{-/-}$*Ripk3*$^{-/-}$ mice experienced prenatal death, which occurred earlier than the death of *A20*$^{-/-}$ mice (**Fig.5 b-c**). These results suggest that the ABIN1-A20 axis through the UBD domain and both FADD and RIPK3 coordinately regulate a vital process during development.

Due to the high expression level of MLKL observed in *Abin1*$^{UBD/UBD}$*Fadd*$^{-/-}$*Ripk3*$^{-/-}$ cells (**Fig.4 i**), we wondered whether the embryonic death of *Abin1*$^{UBD/UBD}$*Fadd*$^{-/-}$*Ripk3*$^{-}$ mice was caused by MLKL activation in an RIPK3-independent manner. However, deletion of *Mlkl* could not prevent the embryonic death of *Abin1*$^{UBD/UBD}$*Fadd*$^{-/-}$*Ripk3*$^{-/-}$ mice (**Fig. 5 d-e, Supplementary Fig.6 c**). These findings suggest that the death of *Abin1*$^{UBD/UBD}$*Fadd*$^{-/-}$*Ripk3*$^{-/-}$ mice was not caused by RIPK3 independent necroptosis. We further explored the reason for the embryonic lethality of *Abin1*$^{UBD/UBD}$*Fadd*$^{-/-}$*Ripk3*$^{-/-}$ mice, and found that the yolk sac of the embryos was intact at E14.5 day (**Supplementary Fig.6 d**). However, the fetal liver of *Abin1*$^{UBD/UBD}$*Fadd*$^{-/-}$*Ripk3*$^{-/-}$ mice was significantly smaller than that of control mice (**Supplementary Fig.6 d**). As the fetal liver is mainly responsible for hematopoietic function at this embryonic stage[31, 32], we assessed fetal liver hematopoiesis. The total number of fetal liver cells in *Abin1*$^{UBD/UBD}$*Fadd*$^{-/-}$*Ripk3*$^{-/-}$ embryos was significantly lower than that in control mice at E13.5; however, there was no significant difference in the number of hematopoietic stem cells (LSK). In contrast, the number of LK cells differentiated from LSK and erythroid lineage cells (Ter119^{+}) was significantly reduced (**Supplementary Fig.6 f**). Hence, *Abin1*$^{UBD/UBD}$*Fadd*$^{-/-}$*Ripk3*$^{-/-}$ mice could die from a fetal defect of early hematopoiesis during embryogenesis. Normal hematopoiesis is markedly affected by cytokine production and release[33, 34, 35]. We proceeded to examine the levels of inflammatory cytokines in embryonic tissues. Based on our results, the levels of TNF-α, IL1β, and IL6 were significantly higher in *Abin1*$^{UBD/UBD}$*Fadd*$^{-/-}$*Ripk3*$^{-/-}$ embryos than control embryos (**Fig. 5f**). Notably, by isolating WT, *Abin1*$^{UBD/UBD}$*Fadd*$^{+/-}$*Ripk3*$^{-/-}$, and *Abin1*$^{UBD/UBD}$*Fadd*$^{-/-}$*Ripk3*$^{-/-}$ MEFs with TNF-α stimulation *in vitro*, we identified the spontaneous activation of the p-IKKε/TBK1 signaling pathway only in *Abin1*$^{UBD/UBD}$*Fadd*$^{-/-}$*Ripk3*$^{-/-}$ cells (**Fig. 5 g, Supplementary Fig. 6 g**), which are required for type I IFN production. Such findings indicate that the ABIN1 UBD domain might regulate pathways producing type I IFN. Upon poly(I:C) transfection, *Abin1*$^{UBD/UBD}$*Fadd*$^{-/-}$*Ripk3*$^{-/-}$ cells also produced more IFN-β and IL-6 than *Fadd*$^{-/-}$*Ripk3*$^{-/-}$ cells (**Supplementary Fig.6 h-j**). We investigated the role of type I IFN in the lethality of *Abin1*$^{UBD/UBD}$*Fadd*$^{-/-}$*Ripk3*$^{-/-}$ embryos. The deletion of *Ifnar*, a type I IFN receptor, could not prevent the embryonic lethality of *Abin1*$^{UBD/UBD}$*Fadd*$^{-/-}$*Ripk3*$^{-/-}$ mice as *Abin1*$^{UBD/UBD}$*Fadd*$^{-/-}$*Ripk3*$^{-/-}$*Ifnar*$^{-/-}$ mice still died at E16.5 (**Fig.5 h-i**). Therefore, we speculated that additional cytokines were involved in the embryonic lethality of *Abin1*$^{UBD/UBD}$*Fadd*$^{-/-}$*Ripk3*$^{-/-}$ embryos. Remarkedly, we found that the lethality of *Abin1*$^{UBD/UBD}$*Fadd*$^{-/-}$*Ripk3*$^{-/-}$ embryos was prevented by the co-deletion of *Ifnar* and *Tnfr1*, even though *Abin1*$^{UBD/UBD}$*Fadd*$^{-/-}$*Ripk3*$^{-/-}$*Ifnar*$^{-/-}$*Tnfr1*$^{-/-}$ mice had a lower weight with splenomegaly (**Fig.5 j-l**). Such findings indicate that

ABIN1 collaborates with FADD and RIPK3 to regulate multiple cytokine production, which is vital for early hematopoiesis during embryogenesis.

ABIN1-A20 axes coordinate with FADD and RIPK3 to regulate the RIPK1-dependent release of multiple cytokines

RIPK1 has been reported to mediate cytokine production in *Casp8*$^{-/-}$*Ripk3*$^{-/-}$ embryos[36, 37, 38]. In addition, the RIPK1 K377R mutant is known to be resistant to Sev infection-induced IRF3 phosphorylation[39, 40]. We investigated whether the ubiquitination of RIPK1 is responsible for cytokine production in the *Fadd*$^{-/-}$*Ripk3*$^{-/-}$ background. By transfecting poly(I:C) into *Fadd*$^{-/-}$*Ripk3*$^{-/-}$*Ripk1*$^{K376R/K376R}$ MDF cells deficient in RIPK1 ubiquitination, we found that the aberrant activation of TBK1/IRF3 signaling in *Fadd*$^{-/-}$*Ripk3*$^{-/-}$*Ripk1*$^{K376R/K376R}$ cells was almost inhibited (**Supplementary Fig.7 a**), suggesting that RIPK1 ubiquitination is indeed critical for inflammatory cytokine production in the *Fadd*$^{-/-}$*Ripk3*$^{-/-}$ background.

As ABIN1 UBD is required for A20 assembly and recruitment to the TNFR1-SC to regulate the ubiquitination of RIPK1, we focused on the mechanisms by which the ABIN1 UBD domain on the *Fadd*$^{-/-}$*Ripk3*$^{-/-}$ background regulates RIPK1 ubiquitination. We stimulated WT, *Abin1*$^{UBD/UBD}$, *Abin1*$^{UBD/UBD}$*Fadd*$^{+/-}$*Ripk3*$^{-/-}$, and *Abin1*$^{UBD/UBD}$*Fadd*$^{-/-}$*Ripk3*$^{-/-}$ cells using poly(I:C) transfection. Indeed, the ubiquitination level of RIPK1 was increased along with the reduction of FADD in *Abin1*$^{UBD/UBD}$*Fadd*$^{-/-}$*Ripk3*$^{-/-}$ cells. However, the cleaved RIPK1 was markedly suppressed in *Abin1*$^{UBD/UBD}$*Fadd*$^{+/-}$*Ripk3*$^{-/-}$ cells and was fully abolished in *Abin1*$^{UBD/UBD}$*Fadd*$^{-/-}$*Ripk3*$^{-/-}$ cells (**Fig.6 a**). These findings indicate that FADD plays a critical role as an adaptor to recruit and activate Casp8, and then cleave ubiquitinated RIPK1. Consistent with this finding, in the absence of FADD and RIPK3, although Casp8 was inactivated, RIPK1 ubiquitination did not occur in *Fadd*$^{-/-}$*Ripk3*$^{-/-}$ cells because ABIN1 was intact (**Supplementary Fig.7 b**). Accordingly, ubiquitinated RIPK1 was markedly increased in the E13.5 embryonic tissue of *Abin1*$^{UBD/UBD}$*Fadd*$^{-/-}$*Ripk3*$^{-/-}$ mice and positively correlated with the level of p-IKKε compared to those of controls (**Fig.6 b**). These data suggest that ABIN1 UBD and FADD-Casp8 as two key regulation compartments to maintain RIPK1 ubiquitination, which is critical for multiple cytokines release.

We proceeded to determine whether the activation of the IKKε/TBK1 signaling pathway is mediated by RIPK1 in *Abin1*$^{UBD/UBD}$*Fadd*$^{-/-}$*Ripk3*$^{-/-}$ or *A20*$^{-/-}$*Fadd*$^{-/-}$*Ripk3*$^{-/-}$ cells. By knocking down RIPK1 and MLKL using siRNA, we found that the spontaneous activation of IKKε/TBK1 signaling was inhibited by RIPK1 knock-down, but not by MLKL knock-down (**Fig. 6 c, Supplementary Fig.7 b**). Such findings imply that the overproduction of multiple cytokines mediated by IKKε/TBK1 signaling in *Abin1*$^{UBD/UBD}$*Fadd*$^{-/-}$*Ripk3*$^{-/-}$ mice could be dependent on RIPK1 in a MLKL independent process. This hypothesis was further supported by our finding that the lethality of *Abin1*$^{UBD/UBD}$*Fadd*$^{-/-}$*Ripk3*$^{-/-}$ and *A20*$^{-/-}$*Fadd*$^{-/-}$*Ripk3*$^{-/-}$ mice was prevented by additional *Ripk1* knockout (**Fig. 6 d-h, Supplementary Fig.7 d-e**), even though *Abin1*$^{UBD/UBD}$*Fadd*$^{-/-}$*Ripk3*$^{-/-}$*Ripk1*$^{-/-}$ and *A20*$^{-/-}$*Fadd*$^{-/-}$*Ripk3*$^{-/-}$*Ripk1*$^{-/-}$ mice were smaller and developed splenomegaly relative to the control littermates (**Supplementary Fig.7 f-i**). We isolated the E14.5 embryo tissue and confirmed that the level of p-IKKε in *Abin1*$^{UBD/UBD}$*Fadd*$^{-/-}$*Ripk3*$^{-/-}$*Ripk1*$^{-/-}$ embryos returned to

normal (**Supplementary Fig.7 j**). Abnormal phenotypes associated with elevated levels of inflammatory cytokines in *Abin1*$^{UBD/UBD}$*Fadd*$^{-/-}$*Ripk3*$^{-/-}$ mice were largely suppressed by the additional deletion of *Ripk1* (**Fig.6 i-j**). These results suggest that the RIPK1-mediated production of multiple inflammatory cytokines was responsible for *Abin1*$^{UBD/UBD}$*Fadd*$^{-/-}$*Ripk3*$^{-/-}$ embryonic lethality. We next evaluated whether RIPK1-mediated production of multiple inflammatory cytokines in *Abin1*$^{UBD/UBD}$*Fadd*$^{-/-}$*Ripk3*$^{-/-}$ mice is dependent on RIPK1 kinase function. In contrast to viable *Abin1*$^{UBD/UBD}$*Fadd*$^{-/-}$*Ripk3*$^{-/-}$*Ripk1*$^{-/-}$ mice, *Abin1*$^{UBD/UBD}$*Fadd*$^{-/-}$*Ripk3*$^{-/-}$*Ripk1*$^{K45A/K45A}$ mice showed growth retardation at the later stage of embryonic development, although some could survive to birth, but also died soon after birth (**Supplementary Fig.8 a-d**). Hence, the lethality of *Abin1*$^{UBD/UBD}$*Fadd*$^{-/-}$*Ripk3*$^{-/-}$ mice is independent of the kinase activity of RIPK1.

Discussion

Multiple genetic studies have strongly associated the genetic polymorphisms of A20 (TNFAIP3) and its binding partner, ABIN1 (TNIP-1), with the incidence and severity of multiple inflammatory and autoimmune diseases[41, 42, 43, 44]. ABIN1 contains a UBD domain that binds to polyubiquitin and polyubiquitinated proteins and a NEMO binding domain (NBD) at the C-terminus. Recent reports have demonstrated that A20 and ABIN1 synergistically regulate NF-κB signaling and cell death pathway[7, 10, 15, 45]. However, the physiological mechanisms by which the UBD domain of ABIN1 regulates these pathways remains unknown.

Mice expressing ABIN1 mutants D485N within UBD domain were reported to be viable, but displayed features of autoimmunity[9, 46, 47], in sharp contrast to the embryonic lethality of *Abin1*$^{-/-}$ mice. As the functions of the ABIN1 UBD domain might not be entirely destroyed by these mutations, the role of the UBD domain of ABIN1 in embryonic development remains unclear. In this study, we generated an ABIN1 mutant mice with the deletion of the UBD domain at positions 452-478 by scissoring exon 13 using the CRISPR/Cas9 technology. The *Abin1*$^{UBD/UBD}$ mice died from excessive fetal liver cell death and hypoplasia, resembling *Abin1* deficient mice, revealing that the UBD domain of ABIN1 is critical for ABIN1 function in the assurance of normal embryonic development.

Furthermore, we demonstrated that the UBD domain of ABIN1 is essential for preventing embryonic lethality caused by TNFR1 signaling (**Fig.1e-f**). We showed that *Abin1*$^{UBD/UBD}$ MEFs were more sensitive to TS- or TC-induced apoptosis and TSZ- or TCZ-induced necroptosis (**Supplementary Fig. 2a-c, 3a-d**). In addition, we found that the mutant ABIN1^{UBD} could not be recruited to TNF-RSC, resulting in the reduced recruitment of A20 and phosphorylated A20, which leads to RIPK1 ubiquitination, activation, and complex II formation-mediated apoptosis and necroptosis (**Supplementary Fig.9b**). Thus, the ABIN1 UBD domain is critical for the assembly and recruitment of A20 to TNF-RSC by recognizing and binding to the ubiquitinated RIPK1, thereby preventing RIPK1 activation-mediated apoptosis and necroptosis.

More importantly, the embryonic lethality of *Abin1*$^{UBD/UBD}$ mice was prevented by *Tnfr1* deficiency, RIPK1 kinase inactive mutant, and co-deletion of RIPK3 with one allele *Fadd* (**Fig.4a-c**). Such findings support the notion that ABIN1 UBD domain is essential for restricting TNFR1 and the RIPK1 kinase activity mediated apoptosis and necroptosis (**Supplementary Fig.9a**). Unexpectedly, *Abin1*$^{UBD/UBD}$*Fadd*$^{+/-}$ *Ripk3*$^{-/-}$ mice died at an earlier gestation stage than *Abin1*$^{UBD/UBD}$ mice and exhibited enhanced production of multiple inflammatory cytokines (**Fig.5e-g; Supplementary Fig.6-f, h**). Similar lethality has also been reported for *Ripk3*$^{-/-}$*Casp8*$^{-/-}$ mice with *Hoil-1*, *Sharpin* mutation, or *OTULIN* enzymatic inactivity mutation[48, 49, 50]. Herein, we also found that *A20*$^{-/-}$*Fadd*$^{+/-}$*Ripk3*$^{-/-}$ mice died shortly after birth. These results indicate that the ABIN1-A20 axis and LUBAC corporately function in a ubiquitin regulation pathway to ensure normal embryogenesis. Two studies speculated that aberrant type I IFN signaling or other cytokines could be responsible for the lethality of triple knockout mice as excessive cytokine production was found in the serum of these mice[49, 50], which is consistent with our observation in *Abin1*$^{UBD/UBD}$*Fadd*$^{+/-}$*Ripk3*$^{-/-}$ mice and *A20*$^{-/-}$*Fadd*$^{+/-}$*Ripk3*$^{-/-}$ mice. Interestingly, our results showed that *Ripk1* deficiency prevented the lethality of *Abin1*$^{UBD/UBD}$*Fadd*$^{+/-}$*Ripk3*$^{-/-}$ mice and *A20*$^{-/-}$*Fadd*$^{+/-}$*Ripk3*$^{-/-}$ mice, consistent with the previous reports that RIPK1 contributed to the earlier lethality of *Ripk3*$^{-/-}$*Casp8*$^{-/-}$*Hoil-1*$^{-/-}$ and *Otulin*$^{C129A/C129A}$ *Ripk3*$^{-/-}$ *Casp8*$^{-/-}$ and [49, 50]. Notably, we further demonstrated that the lethality of *Abin1*$^{UBD/UBD}$*Fadd*$^{+/-}$*Ripk3*$^{-/-}$ mice and *A20*$^{-/-}$*Fadd*$^{+/-}$*Ripk3*$^{-/-}$ mice depends on the scaffolding function of RIPK1, but not on the kinase activity of RIPK1 (**Supplementary Fig.8a-d**). More importantly, we found that *Ifnar*$^{-/-}$ mice did not prevent the lethality of *Abin1*$^{UBD/UBD}$*Fadd*$^{+/-}$*Ripk3*$^{-/-}$ mice (**Fig.5i**). In contrast, *Ifnar*$^{-/-}$*Tnfr1*$^{-/-}$ double knockout mice completely rescued the embryonic lethality of *Abin1*$^{UBD/UBD}$*Fadd*$^{+/-}$ *Ripk3*$^{-/-}$ mice (**Fig.5j-l**). Mechanistically, ABIN1 UBD preserves RIPK1 ubiquitination that was cleaved by activated FADD-Casp8 complex to regulate IKKε/TBK1 pathway mediated the production of multiple inflammatory cytokines (**Fig.6a-c**). Such findings indicate that the ABIN1-A20 axis with LUBAC coordinately serves as a ubiquitin pathway to regulate cell death and production of multiple cytokines, including TNF-α and type I interferon during embryogenesis.

Collectively, our studies uncovered a novel mechanism whereby the ABIN1 UBD domain regulates RIPK1 kinase-mediated cell death and RIPK1 kinase-independent production of multiple cytokines to enable proper development. These new findings reveal an additional mechanism whereby ABIN1 is implicated in the pathogenesis of related human diseases through its UBD domain.

Experimental Procedures

Mice. All mice were housed in a specific pathogen-free (SPF) facility at Shanghai Institute of Nutrition and Health, Chinese Academy of Sciences. *Fadd*$^{+/-}$ mice were gifted by Dr. Jianke Zhang (Thomas Jefferson University, Philadelphia, USA), and *Rip3*$^{-/-}$ mice were provided by Dr. Xiaodong Wang (NIBS, Beijing, China). *Ripk1*$^{-/-}$, *Ripk1*$^{K45A/K45A}$, *Mlkl*$^{-/-}$, *Tnfr1*$^{-/-}$, *and Ifnar*$^{-/-}$ mouse lines have been described previously[24, 51]. *A20*$^{-/-}$ mice were generated using the CRISPR/Cas9 mutation system (Bioray Laboratories Inc., Shanghai, China). *Abin1*$^{UBD/UBD}$ mice were generated by a 110 bp deletion in the coding region of

exon 13 and following the intron region using the CRISPR-Cas9 mutation system. *Abin1*$^{UBD/UBD}$ mouse genotyping primers (ABIN1-F: 5'-TCAGTGCAGCGGTAATGAGT-3' and ABIN1-R: 5'-ATACATGCAGGCAGAACACT-3') amplified 414 bp wild-type and 304 bp ABIN1^{UBD} DNA fragments. All newly constructed mouse lines were backcrossed onto the C57BL/6 background for more than five generations. Animal experiments were conducted in accordance with the guidelines of the Institutional Animal Care and Use Committee of the Shanghai Institute of Nutrition and Health, University of Chinese Academy of Sciences, Chinese Academy of Sciences.

Reagents. Western blotting antibodies: RIPK1 (1:2000, Cell Signaling Technology, 3493P), p-RIPK1(1:1000, Cell Signaling Technology, 31122S), RIPK3 (1:5000, Prosci, 2283), p-RIPK3 (1:1000, homemade), MLKL (1:1000, Abgent, ap14272b), p-MLKL (1:1000, Abcam, ab196436), FADD (1:1000, Abcam, ab124812), ABIN1 (1:2000, Proteintech, 15104-1-AP), ABIN1 (1:1000, Invitrogen, PA5-83395), A20 (1:1000, Cell Signaling Technology, 5630S), p-A20 (1:1000, Cell Signaling Technology, 63523S), CYLD (1:1000, Cell Signaling Technology, 8462S), SHARPIN (1:2000, Proteintech, 14626-1-AP), TAK1 (1:1000, Cell Signaling Technology, 5206S), TRADD (1:1000, Cell Signaling Technology, 3694S), NEMO (1:200, Cell Signaling Technology, 2685S), GAPDH (1:20000, Sigma, G9545), ACTIN (1:10000,Sigma, A3854), PARP (1:1000, Cell Signaling Technology, 9542S), Caspase-3 (1:1000, Cell Signaling Technology, 9662S), Cleaved Caspase-3 (1:1000, Cell Signaling Technology, 9661S), K63 (1:1000, Cell Signaling Technology, 5621S), Caspase-8 (1:1000, ENZO, ALX-804-447-C100), Cleaved Caspase-8 (1:1000, Cell Signaling Technology, 9429S), TBK1 (1:1000, Cell Signaling Technology, 3013S), p-TBK1 (1:1000, Cell Signaling Technology, 5483S), IKKε (1:1000, Cell Signaling Technology, 3416), p-IKKε (1:500, Cell Signaling Technology, 8766S), IRF3 (1:1000, Cell Signaling Technology, 4302S), and p-IRF3 (1:1000, Cell Signaling Technology, 4947S). The Smac mimetic and poly(I:C) were purchased from Sigma. TNF-α (410-MT-050) was procured from R&D. Nec-1, BV6, and z-VAD were purchased from MCE. ISD (tlrl-isdn) and cGAMP (tlrl-nacga23-02) were purchased from Invivogen. Flag-beads (A2220) were purchased from Sigma. K63-TUBE (UM604), M1-TUBE (UM606), and ub-TUBE (UM402) were procured from Lifesensors. Flag-TNF-α (ALX-522-009-C050) was purchased from ENZO.

Cell culture. All primary MEFs were from E13.5 or E14.5 embryos (except *Ripk1*$^{K376R/K376R}$ MEFs from E10.5 embryos). Primary MEFs were cultured in high-glucose Dulbecco's modified Eagle's medium (Hyclone, SH30243.LS) supplemented with 10% fetal bovine serum, 2 mM glutamine, 1% penicillin, and 100 μg/ml streptomycin. For immortalization, primary MEFs were transfected with the SV40-T plasmid (Addgene, 22298) using Lipofectamine 3000 (Invitrogen, L3000001) according to the manufacturer's instructions. Primary mouse dermal fibroblasts (MDFs) were separated from the skin of newborn mice. HEK293T cells were cultured in complete DMEM.

Western blotting and immunoprecipitation Cell pellets and embryos were lysed in RIPA lysis buffer containing 50 mM Tris (pH=8.0), 1 mM EDTA, 150 mM NaCl, 0.1% SDS, 1% Triton X-100, 0.2% sodium deoxycholate, 50 mM NaF, 1x proteinase inhibitor cocktail (Roche, 5056489001), 2 mM PMSF, and 5 mM NEM. The protein concentration in the collected supernatants was determined using a BCA protein assay kit (Thermo Scientific, 23225). The normalized lysates were subsequently denatured in reducing 5x SDS

loading sample buffer at 100 °C for 5 min. In figure 1 D, embryos were first homogenized in NP-40 buffer (0.5% NP-40, pH 7.5, 120 mM NaCl, 10% glycerol, 30 mM Tris, 1 mM EDTA, 2 mM KCl, 50 mM NaF, 5 mM sodium pyrophosphate, 10 mM β-glycerophosphate, 2 mM PMSF, 10 mM NEM, and 1x proteinase inhibitor cocktail). After centrifugation, supernatants were normalized as the NP-40 fraction. The pellets were washed with 1x PBS twice, resuspended in 6 M urea lysis buffer (6 M urea, 1% Triton X-100, pH 7.5, 120 mM NaCl, 30 mM Tris, 1 mM EDTA, 2 mM KCl, 50 mM NaF, 5 mM sodium pyrophosphate, 10 mM β-glycerophosphate, 2 mM PMSF, 10 mM NEM, and 1x proteinase inhibitor cocktail), and lysed at 4 ℃ for 1 h. The resulting supernatant was the 6 M urea fraction.

For TNF-RSC immunoprecipitation, immortalized MEFs were stimulated with flag-TNF-α (100 ng/ml) for the indicated time. Cells were washed twice with ice-cold 1x PBS and subsequently lysed in NP-40 buffer at 4 °C for 1 h with rotation. The lysates were cleared by centrifugation and then incubated with FLAG-tagged beads (Sigma, A2220) for 16 h. Complex II was immunoprecipitated by overnight incubation with RIPK1 (BD, 610459) antibody at 4 °C with rotation, followed by 6 h incubation with protein A/G resin (Thermo Scientific, 53133). The beads were washed with ice-cold NP-40 buffer at least three times. Proteins were eluted with 40 μl 2x SDS loading sample buffer.

For TUBE pull-down, cells were stimulated with TNF-α at indicated time, and lysed with TUBE lysis buffer (100 mM Tris-HCl, pH 8.0, 0.15 M NaCl, 5 mM EDTA, 1% NP-40, 0.5% Triton-X 100, 2 mM NEM, 50 μM PR619, 2 mM o-PA, protein inhibitor cocktail, 5 mM PMSF and 150 nM flag-TUBE) at 4 ℃ for 30 min. The lysates were cleared by centrifugation and then diluted ten-fold in dilution buffer (100 mM Tris-HCl, pH 8.0, 0.15M NaCl, 5 mM EDTA, 2 mM NEM, 50 μM PR619, 2 mM o-PA, protein inhibitor cocktail, 5 mM PMSF, and 150 nM flag-TUBE). Flag-TUBEs were pulled down with anti-flag beads overnight at 4 °C, and then washed with cold wash buffer (100 mM Tris-HCl, pH 8.0, 0.15 M NaCl, 5 mM EDTA, 0.05% NP-40). Finally, 20 μl of 5x SDS reducing loading sample buffer was added to the resin, and the sample was heated at 96 °C for 5 min.

Cell viability assay. Cells were seeded to 80% confluence in 96-well plates and treated with 20 ng/ml TNF-α, 30 μM Nec-1, 20 μM zVAD, and other stimuli at the indicated time. Cell viability was measured using the CellTiter-Glo Luminescent Cell Viability Assay kit (Promega, G7572), according to the manufacturer's instructions.

Flow analysis. Single-cell suspensions from the spleen and mesenteric lymph nodes were stained with various fluorophore-conjugated antibody cocktails. These antibodies included CD3-FITC (BD, 553061), B220-PE (eBioscience, 12-0452-83), CD4-APC-CY7 (BD, 552051), CD8-PerCP (BioLegend, 100732), CD62L-PE-CY7 (eBioscience, 25-0621-81), CD44-APC (eBioscience, 17-0441-81), Ly6G/C-PE (eBioscience, 12-5931-83), and CD11B-APC (eBioscience, 17-0112-82). For fetal liver LSK staining, single-cell suspensions from mechanically dissociated E13.5 embryos' fetal livers were stained with antibodies against: Scal1-APC (eBioscience, 17-5981-82), cKit-APC-eFluor780 (eBioscience, 47-1172-82), Strepavidin-PE-CY7 (Invitrogen, SA1012), biotin-conjugated: CD3 (eBioscience, 13-0032-80), CD4 (eBioscience, 13-0041-81), CD5 (eBioscience, 13-0051-81), CD8 (eBioscience, 13-0081-81), B220 (eBioscience, 13-0452-81), CD19

(eBioscience, 13-0193-81), Ly6G (eBioscience, 13-5931-81), CD11B (eBioscience, 13-0112-81), and Ter119 (eBioscience, 13-5921-81). Samples were acquired on FACS Aria II (BD Biosciences) and analyzed using FlowJo software.

Cytokine assay. Embryo homogenates lysed with RIPA buffer and cell supernatants were assayed using TNF-α (eBioscience, 88-7324-88), IL-1β (eBioscience, 88-7013-88), IL-6 (eBioscience, 88-7064-88), IFN-β (PBL, 424001), IFN-β (Biolegend, 439407) ELISA kit.

siRNA transfection. All siRNAs were transfected using Lipofectamine RNAiMAX transfection reagent (Invitrogen, 13778-150). The siRNA sequences included: *Ripk1* 5'-GAAUGAGGCUUACAACAGA-3'; and *Mlkl* 5'-GAGAUCCAGUUCAACGAUA-3'.

Immunohistochemistry and TUNEL staining Embryonic livers were fixed in 4% paraformaldehyde for hematoxylin and eosin staining, immunohistochemistry**,** and TUNEL staining. For immunohistochemistry, cleaved Caspase-3 was labeled with rabbit anti-cleaved Caspase-3 (9661, CST).

Statistics and Reproducibility The data presented in this article were obtained independently at least thrice. The statistical significance of data was evaluated by unpaired two-tailed Student's *t-test*. Statistical calculations and graphs were generated using the GraphPad Prism 8 software.

Declarations

SUPPLEMENTARY INFORMATION

Supplementary information includes nine figures.

AUTHOR CONTRIBUTIONS

M.L and H.B.Z designed the study; M.L performed all experiments and analyzed data with assistance from J.L.L, M.Y.X, X.M.L, H.W.Z, X.X.W, L.X.W, Y.J.O, X.H.W, X.M.Z, H.L, F.L, W.W.R, J.S.D, X.Z.W. and Z.C.W; Y.B.L analyzed *A20*$^{-/-}$ *Ripk3*$^{-/-}$*Fadd*$^{+/-}$ mice; C.X.X and Q.Z analyzed *Abin1*$^{UBD/UBD}$ mice; J.B.L, Y.W.Z, A.K.L and Q.F.L provided resources and intellectual input. M.L and H.B.Z assembled figure panels and wrote the paper. H.B.Z supervised the project.

ACKNOWLEDGEMENTS

We thank Dr. Xiaodong Wang (National Institute of Biological Sciences, Beijing, China) for providing *Ripk3*$^{-/-}$ mice, Dr. Jianke Zhang (Thomas Jefferson University, Philadelphia, PA, USA) for providing *Fadd*$^{+/-}$ mice, Dr. Feng Shao (National Institute of Biological Sciences, Beijing, China) for providing *Tnfr1*$^{-/-}$ mice and Dr. Qibin Leng (Institute Pasteur of Shanghai, Shanghai, China) for providing *Ifnar*$^{-/-}$ mice. We also thank Lin Qiu for flow cytometry technical assistance. We thank Dr. Yu Sun (UCLA, Los Angeles, California) for editing of the manuscript and helpful discussions. This work was supported by grants from the National Key Research and Development Program of China (2018YFC1200201,

2016YFC1304900) and the National Natural Science Foundation of China (31970688, 31771537, 82071288, 82001684). Z.C.W was supported by “Chenguang Program” of Shanghai Education Development Foundation (19CG18) and Shanghai Rising Star Program of Science and Technology Commission of Shanghai Municipality (20QA1405600).

CONFLIC OF INTEREST

The authors declare no competing interests.

References

1. Gateva, V. *et al.* A large-scale replication study identifies TNIP1, PRDM1, JAZF1, UHRF1BP1 and IL10 as risk loci for systemic lupus erythematosus. *Nature genetics* **41**, 1228–1233 (2009).
2. Han, J.W. *et al.* Genome-wide association study in a Chinese Han population identifies nine new susceptibility loci for systemic lupus erythematosus. *Nature genetics* **41**, 1234–1237 (2009).
3. He, C.F. *et al.* TNIP1, SLC15A4, ETS1, RasGRP3 and IKZF1 are associated with clinical features of systemic lupus erythematosus in a Chinese Han population. *Lupus* **19**, 1181–1186 (2010).
4. Heyninck, K. *et al.* The zinc finger protein A20 inhibits TNF-induced NF-kappaB-dependent gene expression by interfering with an RIP- or TRAF2-mediated transactivation signal and directly binds to a novel NF-kappaB-inhibiting protein ABIN. *The Journal of cell biology* **145**, 1471–1482 (1999).
5. Callahan, J.A. *et al.* Cutting edge: ABIN-1 protects against psoriasis by restricting MyD88 signals in dendritic cells. *Journal of immunology (Baltimore, Md.*: 1950) **191**, 535–539 (2013).
6. Caster, D.J. *et al.* ABIN1 dysfunction as a genetic basis for lupus nephritis. *Journal of the American Society of Nephrology: JASN* **24**, 1743–1754 (2013).
7. Mauro, C. *et al.* ABIN-1 binds to NEMO/IKKgamma and co-operates with A20 in inhibiting NF-kappaB. *The Journal of biological chemistry* **281**, 18482–18488 (2006).
8. Gao, L. *et al.* ABIN1 protein cooperates with TAX1BP1 and A20 proteins to inhibit antiviral signaling. *The Journal of biological chemistry* **286**, 36592–36602 (2011).
9. Nanda, S.K. *et al.* Polyubiquitin binding to ABIN1 is required to prevent autoimmunity. *The Journal of experimental medicine* **208**, 1215–1228 (2011).
10. Oshima, S. *et al.* ABIN-1 is a ubiquitin sensor that restricts cell death and sustains embryonic development. *Nature* **457**, 906–909 (2009).
11. Wagner, S. *et al.* Ubiquitin binding mediates the NF-kappaB inhibitory potential of ABIN proteins. *Oncogene* **27**, 3739–3745 (2008).
12. Skaug, B. *et al.* Direct, noncatalytic mechanism of IKK inhibition by A20. *Molecular cell* **44**, 559–571 (2011).
13. Wertz, I.E. *et al.* Phosphorylation and linear ubiquitin direct A20 inhibition of inflammation. *Nature* **528**, 370–375 (2015).

14. Lu, T.T. *et al.* Dimerization and ubiquitin mediated recruitment of A20, a complex deubiquitinating enzyme. *Immunity* **38**, 896–905 (2013).
15. Dziedzic, S.A. *et al.* ABIN-1 regulates RIPK1 activation by linking Met1 ubiquitylation with Lys63 deubiquitylation in TNF-RSC. *Nature cell biology* **20**, 58–68 (2018).
16. Onizawa, M. *et al.* The ubiquitin-modifying enzyme A20 restricts ubiquitination of the kinase RIPK3 and protects cells from necroptosis. *Nature immunology* **16**, 618–627 (2015).
17. Su, Z. *et al.* ABIN-1 heterozygosity sensitizes to innate immune response in both RIPK1-dependent and RIPK1-independent manner. *Cell death and differentiation* **26**, 1077–1088 (2019).
18. Maelfait, J. *et al.* A20 (Tnfaip3) deficiency in myeloid cells protects against influenza A virus infection. *PLoS pathogens* **8**, e1002570 (2012).
19. Parvatiyar, K., Barber, G.N. & Harhaj, E.W. TAX1BP1 and A20 inhibit antiviral signaling by targeting TBK1-IKKi kinases. *The Journal of biological chemistry* **285**, 14999–15009 (2010).
20. Zhou, J. *et al.* A20-binding inhibitor of NF-κB (ABIN1) controls Toll-like receptor-mediated CCAAT/enhancer-binding protein β activation and protects from inflammatory disease. *Proceedings of the National Academy of Sciences of the United States of America* **108**, E998-1006 (2011).
21. Degterev, A. *et al.* Chemical inhibitor of nonapoptotic cell death with therapeutic potential for ischemic brain injury. *Nature chemical biology* **1**, 112–119 (2005).
22. Li, W. *et al.* BV6, an IAP antagonist, activates apoptosis and enhances radiosensitization of non-small cell lung carcinoma in vitro. *Journal of thoracic oncology: official publication of the International Association for the Study of Lung Cancer* **6**, 1801–1809 (2011).
23. Newton, K. *et al.* RIPK1 inhibits ZBP1-driven necroptosis during development. *Nature* **540**, 129–133 (2016).
24. Zhang, X. *et al.* Ubiquitination of RIPK1 suppresses programmed cell death by regulating RIPK1 kinase activation during embryogenesis. *Nature communications* **10**, 4158 (2019).
25. Tang, Y. *et al.* K63-linked ubiquitination regulates RIPK1 kinase activity to prevent cell death during embryogenesis and inflammation. *Nature communications* **10**, 4157 (2019).
26. Kist, M. *et al.* Impaired RIPK1 ubiquitination sensitizes mice to TNF toxicity and inflammatory cell death. *Cell death and differentiation* **28**, 985–1000 (2021).
27. Hutti, J.E. *et al.* IkappaB kinase beta phosphorylates the K63 deubiquitinase A20 to cause feedback inhibition of the NF-kappaB pathway. *Molecular and cellular biology* **27**, 7451–7461 (2007).
28. Wertz, I.E. *et al.* De-ubiquitination and ubiquitin ligase domains of A20 downregulate NF-kappaB signalling. *Nature* **430**, 694–699 (2004).
29. Boone, D.L. *et al.* The ubiquitin-modifying enzyme A20 is required for termination of Toll-like receptor responses. *Nature immunology* **5**, 1052–1060 (2004).
30. Newton, K. *et al.* RIPK3 deficiency or catalytically inactive RIPK1 provides greater benefit than MLKL deficiency in mouse models of inflammation and tissue injury. *Cell death and differentiation* **23**, 1565–1576 (2016).

31. Cumano, A. & Godin, I. Ontogeny of the hematopoietic system. *Annual review of immunology* **25**, 745–785 (2007).
32. McGrath, K.E. *et al.* A transient definitive erythroid lineage with unique regulation of the β-globin locus in the mammalian embryo. *Blood* **117**, 4600–4608 (2011).
33. Yockey, L.J. & Iwasaki, A. Interferons and Proinflammatory Cytokines in Pregnancy and Fetal Development. *Immunity* **49**, 397–412 (2018).
34. Clapes, T., Lefkopoulos, S. & Trompouki, E. Stress and Non-Stress Roles of Inflammatory Signals during HSC Emergence and Maintenance. *Frontiers in immunology* **7**, 487 (2016).
35. Pietras, E.M. Inflammation: a key regulator of hematopoietic stem cell fate in health and disease. *Blood* **130**, 1693–1698 (2017).
36. Kang, T.B., Jeong, J.S., Yang, S.H., Kovalenko, A. & Wallach, D. Caspase-8 deficiency in mouse embryos triggers chronic RIPK1-dependent activation of inflammatory genes, independently of RIPK3. *Cell death and differentiation* **25**, 1107–1117 (2018).
37. Rickard, J.A. *et al.* RIPK1 regulates RIPK3-MLKL-driven systemic inflammation and emergency hematopoiesis. *Cell* **157**, 1175–1188 (2014).
38. Dillon, C.P. *et al.* RIPK1 blocks early postnatal lethality mediated by caspase-8 and RIPK3. *Cell* **157**, 1189–1202 (2014).
39. Rajput, A. *et al.* RIG-I RNA helicase activation of IRF3 transcription factor is negatively regulated by caspase-8-mediated cleavage of the RIP1 protein. *Immunity* **34**, 340–351 (2011).
40. Liu, Z. & Chan, F.K. Regulatory mechanisms of RIPK1 in cell death and inflammation. *Seminars in cell & developmental biology* **109**, 70–75 (2021).
41. Malynn, B.A. & Ma, A. A20: A multifunctional tool for regulating immunity and preventing disease. *Cellular immunology* **340**, 103914 (2019).
42. Catrysse, L., Vereecke, L., Beyaert, R. & van Loo, G. A20 in inflammation and autoimmunity. *Trends in immunology* **35**, 22–31 (2014).
43. Schuijs, M.J. *et al.* Farm dust and endotoxin protect against allergy through A20 induction in lung epithelial cells. *Science (New York, N.Y.)* **349**, 1106–1110 (2015).
44. Zhou, Q. *et al.* Loss-of-function mutations in TNFAIP3 leading to A20 haploinsufficiency cause an early-onset autoinflammatory disease. *Nature genetics* **48**, 67–73 (2016).
45. Kattah, M.G. *et al.* A20 and ABIN-1 synergistically preserve intestinal epithelial cell survival. *The Journal of experimental medicine* **215**, 1839–1852 (2018).
46. Nanda, S.K., Lopez-Pelaez, M., Arthur, J.S., Marchesi, F. & Cohen, P. Suppression of IRAK1 or IRAK4 Catalytic Activity, but Not Type 1 IFN Signaling, Prevents Lupus Nephritis in Mice Expressing a Ubiquitin Binding-Defective Mutant of ABIN1. *Journal of immunology (Baltimore, Md.*: 1950) **197**, 4266–4273 (2016).
47. Nanda, S.K. *et al.* Distinct signals and immune cells drive liver pathology and glomerulonephritis in ABIN1[D485N] mice. *Life science alliance* **2** (2019).

48. Rickard, J.A. *et al.* TNFR1-dependent cell death drives inflammation in Sharpin-deficient mice. *eLife* **3** (2014).
49. Peltzer, N. *et al.* LUBAC is essential for embryogenesis by preventing cell death and enabling haematopoiesis. *Nature* **557**, 112–117 (2018).
50. Heger, K. *et al.* OTULIN limits cell death and inflammation by deubiquitinating LUBAC. *Nature* **559**, 120–124 (2018).
51. Liu, Y. *et al.* RIP1 kinase activity-dependent roles in embryonic development of Fadd-deficient mice. *Cell death and differentiation* **24**, 1459–1469 (2017).

Figures

Figure 1

a

Stage	E13.5	E14.5	E15.5	E16.5	E17.5	Weaned
Abin1$^{+/+}$	5	8	4	10	7	62
Abin1$^{+/UBD}$	9	10	19	10	19	100
Abin1$^{UBD/UBD}$	9	6	9	8*	7*	0
Sum	23	24	32	28	33	162

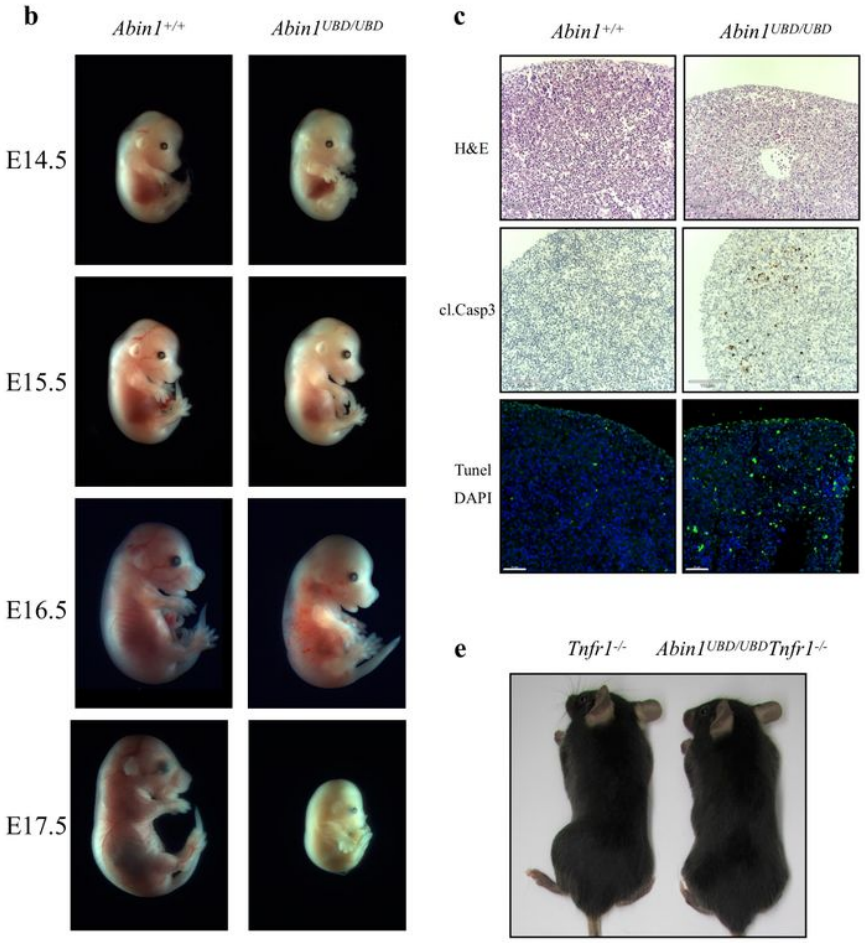

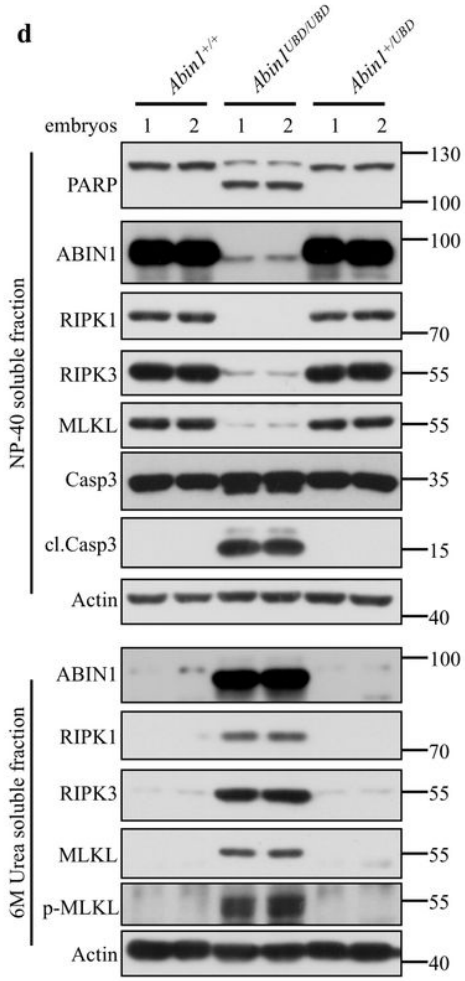

f

Stage	Weaned
Abin1$^{+/+}$*Tnfr1*$^{-/-}$	8
Abin1$^{+/UBD}$*Tnfr1*$^{-/-}$	19
Abin1$^{UBD/UBD}$*Tnfr1*$^{-/-}$	10
Sum	37

Figure 1

The ABIN1UBD mutants caused embryonic lethality due to aberrant TNFR1-mediated cell death. a. Embryo or offspring counts from different periods for Abin1UBD/+ mice intercrosses. * Indicated abnormal embryos. b. Representative images of embryos with the indicated genotypes from E14.5 to E17.5. c. Microscopic images of H&E, cleaved Caspase-3, and TUNEL staining in liver sections with indicated genotypes at E16.5 (scale bar, 110 μm for H&E and cleaved Caspase-3 staining, 50 μm for TUNEL staining). d. Western blotting analyses of different lysate fractions of whole embryos with the indicated genotypes from E16.5. e. Representative macroscopic images of Tnfr1-/- and Abin1UBD/UBDTnfr1-/- mice at 2 months. f. Offspring counts at weaning from crosses of Abin1UBD/+Tnfr1-/- mice.

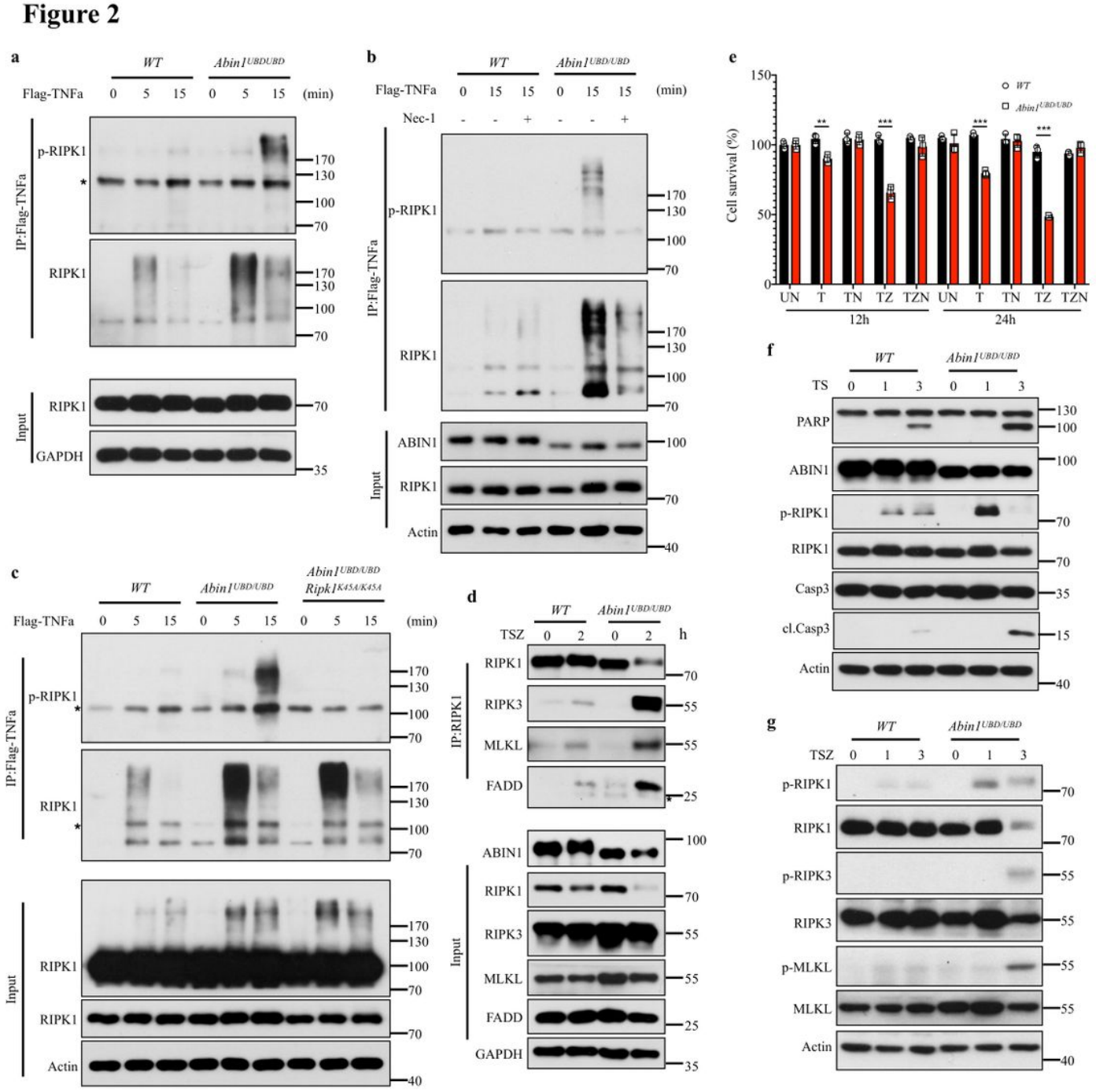

Figure 2

The UBD domain of ABIN1 suppresses RIPK1 activation in TNF-RSC. a-b. WT and Abin1UBD/UBD immortal MEFs were treated with Flag-TNF-α (100 ng/ml) for the indicated time, and the TNFR1 complex (TNF-RSC) was immunoprecipitated using anti-Flag beads. RIPK1 ubiquitination and phosphorylation were detected using western blotting. nec-1 was added to the selected samples, as indicated. c. WT, Abin1UBD/UBD, and Abin1UBD/UBDRipk1K45A/K45A immortal MEFs were stimulated with Flag-TNF-α (100 ng/ml) for the indicated time, and the TNFR1 complex was immunoprecipitated using anti-Flag resin. RIPK1 ubiquitination and phosphorylation were detected by western blotting using anti-RIPK1 and

anti-p-RIPK1(Ser166) antibodies. d. WT and Abin1UBD/UBD immortalized MEFs were treated with mouse T (TNF-α, 20 ng/ml), S (Smac, 1 μM), and Z (Zvad, 20 μM) for 2 h. Necrosome (complex II) was immunoprecipitated using the anti-RIPK1 antibody, and the components were analyzed by western blotting with the indicated antibodies. For (a-d), * indicates non-specific bands. e. The cell survival of WT and Abin1UBD/UBD immortal MEFs given the indicated stimulations for 12 and 24 h. P values were determined using a two-tailed Student's t-test, * $P<0.05$, ** $P< 0.01$, *** $P<0.001$. f-g. WT and Abin1UBD/UBD immortalized MEFs were stimulated by TS (f) or TSZ (g) at the indicated time, and the apoptosis and necroptosis signaling components were analyzed by western blotting using specific antibodies.

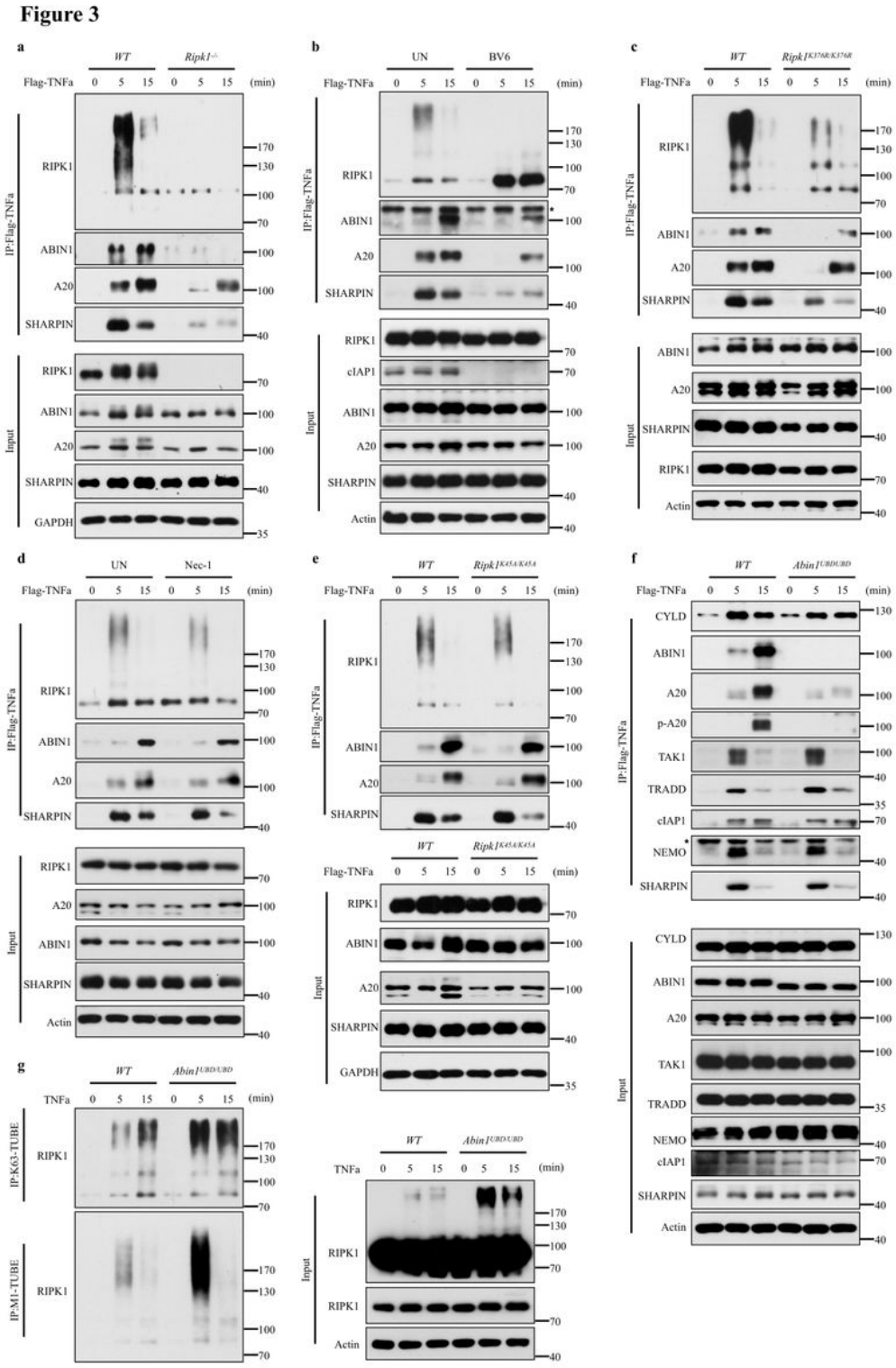

Figure 3

ABIN1 recruits A20 to TNF-RSC by recognizing and binding to the ubiquitinated RIPK1 (a, c, e). TNF-RSC was pulled-down by Flag-beads in immortalized MEFs using the indicated genotypes and analyzed by western blot using anti-RIPK1, anti-ABIN1, anti-A20, and anti-SHARPIN. (b, d). WT MEFs were pretreated with BV6 (0.5 μM) or Nec-1 (30 μM) for 6 h. TNF-RSC was analyzed by western blot using a specific antibody. f. TNF-RSC was immunoprecipitated using anti-Flag beads in WT and Abin1UBD/UBD

immortalized MEFs stimulated by flag-TNF-α (100 ng/ml) for the indicated time. g. Immortalized WT and Abin1UBD/UBD MEFs were stimulated with TNF-α (20 ng/ml) for the indicated time. K63-linked and M1-linked proteins were immunoprecipitated using K63-TUBEs and M1-TUBEs, respectively.

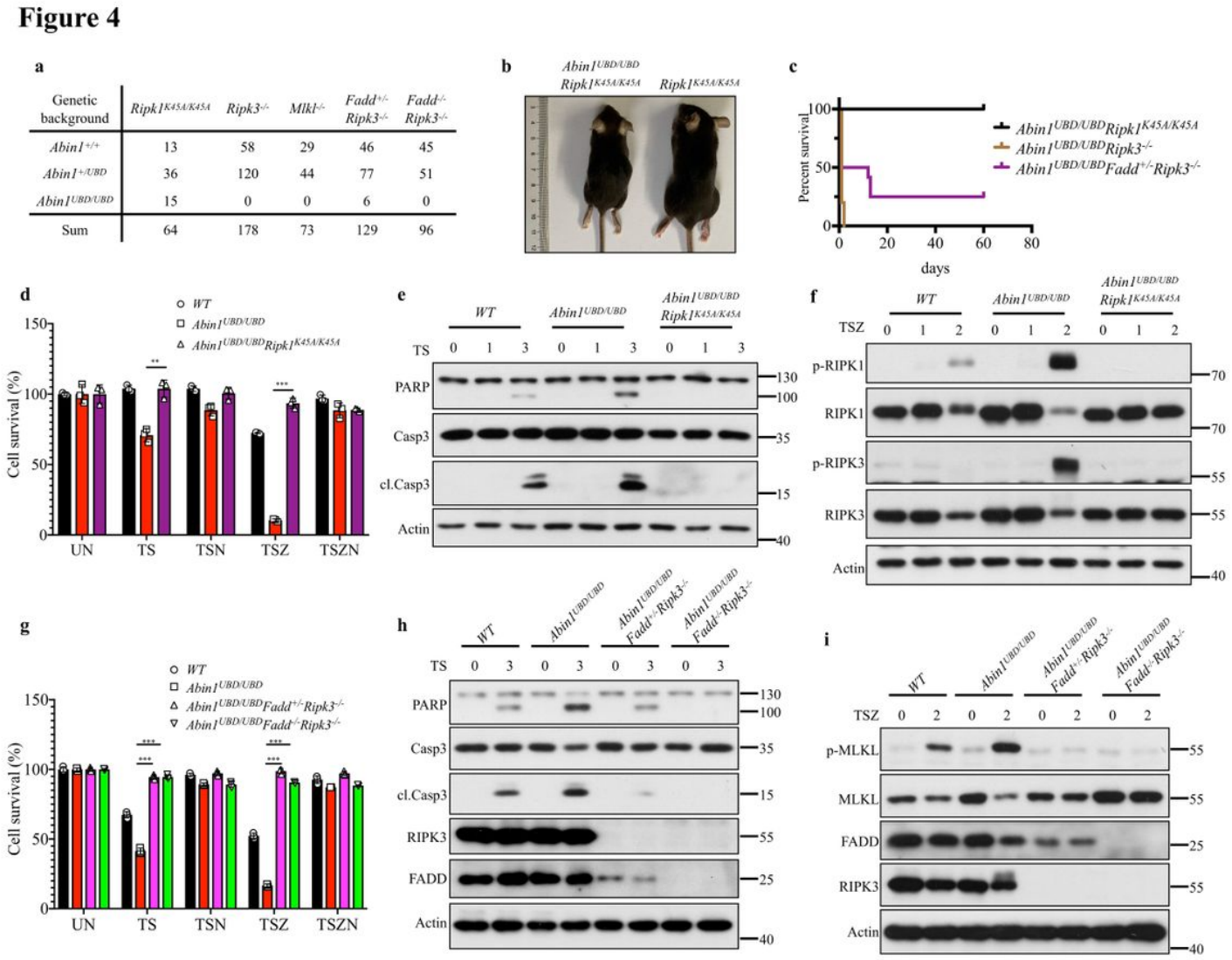

Figure 4

Abin1UBD/UBD mice died from RIPK1 kinase-dependent apoptosis and necroptosis. a. Offspring numbers from intercrossing Abin1UBD/+ mice at weaning in the genetic background as indicated. b. Representative macroscopic images of Abin1UBD/UBDRipk1K45A/K45A and Ripk1K45A/K45A mice at 2 months. c. Survival curves of Abin1UBD/UBDRipk1K45A/K45A (n=6), Abin1UBD/UBDRipk3-/-(n=10), and Abin1UBD/UBDFadd+/-Ripk3-/-(n=12) mice. d. The cell survival of WT, Abin1UBD/UBD, and Abin1UBD/UBDRipk1K45A/K45A immortalized MEFs treated with the indicated stimulations for 3 h. (e-f). WT, Abin1UBD/UBD, and Abin1UBD/UBDRipk1K45A/K45A immortalized MEFs were treated with TS (e) or TSZ (f) for the indicated times, and apoptosis and necroptosis signaling components were analyzed by western blotting using specific antibodies. g. The cell survival of WT, Abin1UBD/UBD, Abin1UBD/UBDFadd+/-Ripk3-/-, and Abin1UBD/UBDFadd-/-Ripk3-/- immortalized MEFs treated with the

indicated stimulations for 4 h. (h-i). WT, Abin1UBD/UBD, Abin1UBD/UBDFadd+/-Ripk3-/-, and Abin1UBD/UBDFadd-/-Ripk3-/- immortalized MEFs were treated with TS (h) or TSZ (i) for the indicated times, and the apoptosis and necroptosis signaling components were analyzed by western blotting using specific antibodies. T (TNF-α, 20 ng/ml), S (Smac, 1 μM), Nec-1 (30 μM), and Z (Zvad, 20 μM). P values were determined using a two-tailed Student's t-test, * P<0.05, ** P< 0.01, *** P<0.001.

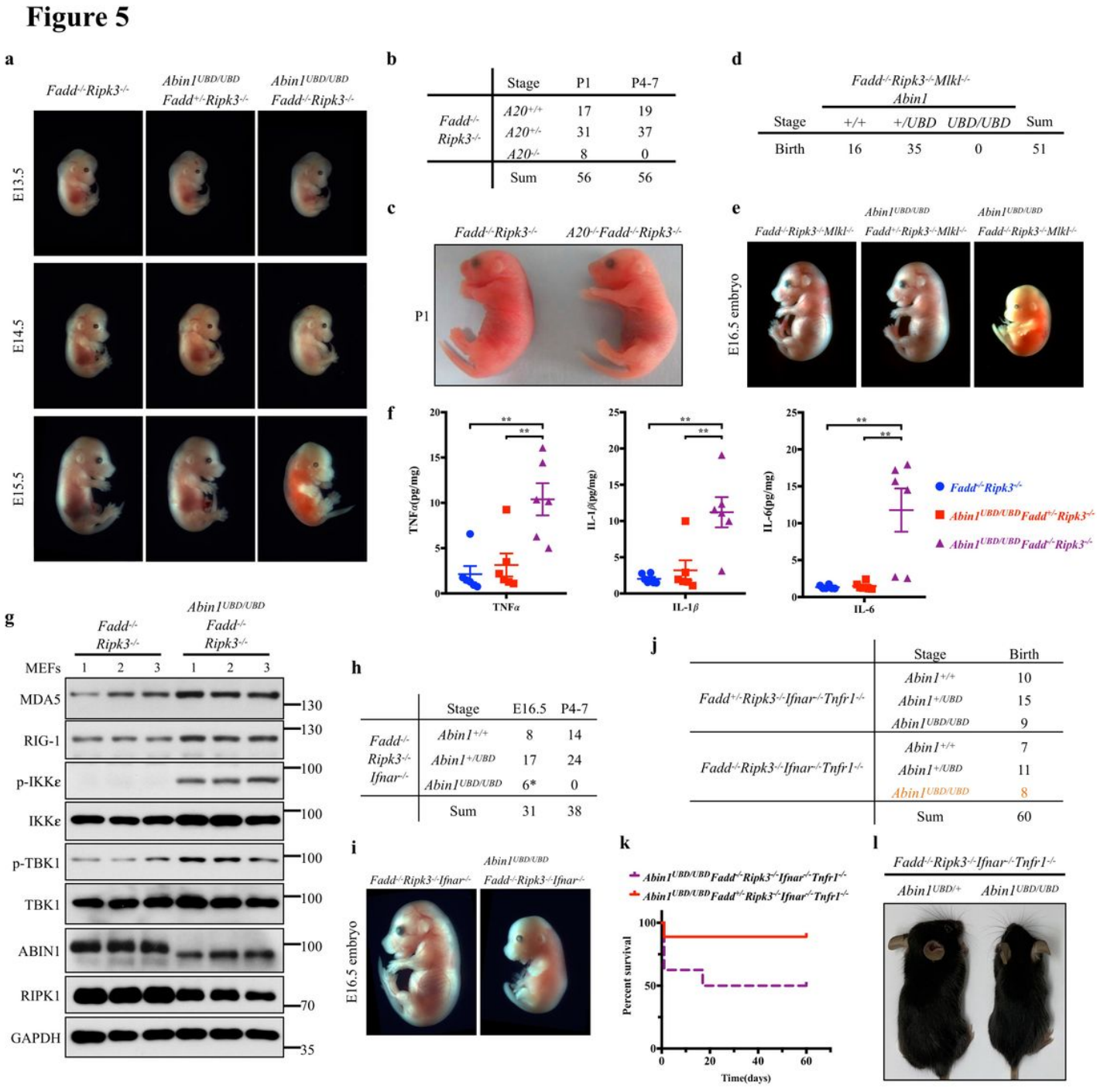

Figure 5

Abin1UBD/UBDFadd-/-Ripk3-/- mice died at mid-gestation with aberrant inflammation. a. Representative images of embryos with the indicated genotypes from E13.5 to E15.5. b. Offspring counts from different periods for the A20+/-Fadd-/-Ripk3-/- mouse intercrosses. c. Representative images of the P1 (1 d after birth) mice quantified in (b). d. Offspring counts from Abin1UBD/+Fadd-/-Ripk3-/-Mlkl-/- mice intercrossed at birth. e. Representative images of embryos with the indicated genotypes at E16.5. f. Cytokines in the embryo homogenate at E15.5, with the indicated genotypes (n=6 embryos per genotype). Data represent mean± SEM; P values were determined using two-tailed Student's t-test, * P<0.05, ** P< 0.01, *** P<0.001. g. Western blot of primary MEFs with the indicated genotypes. h. Embryo or offspring counts from different periods for Abin1UBD/+Fadd-/-Ripk3-/-Ifnar-/- mouse intercrosses. * Indicates the dead embryos. i. Representative images of embryos with the indicated genotypes at E16.5. j. P4-7 offspring numbers from intercrossing Abin1UBD/+Fadd-/-Ripk3-/-Ifnar-/-Tnfr1-/-(male) with Abin1UBD/+Fadd+/-Ripk3-/-Ifnar-/-Tnfr1-/-(female) mice. k. Survival curves of Abin1UBD/UBDFadd+/-Ripk3-/-Ifnar-/-Tnfr1-/- (n=9) and Abin1UBD/UBDFadd-/-Ripk3-/-Ifnar-/-Tnfr1-/- (n=8) mice. l. Representative macroscopic images of the eight-week-old littermates.

Figure 6

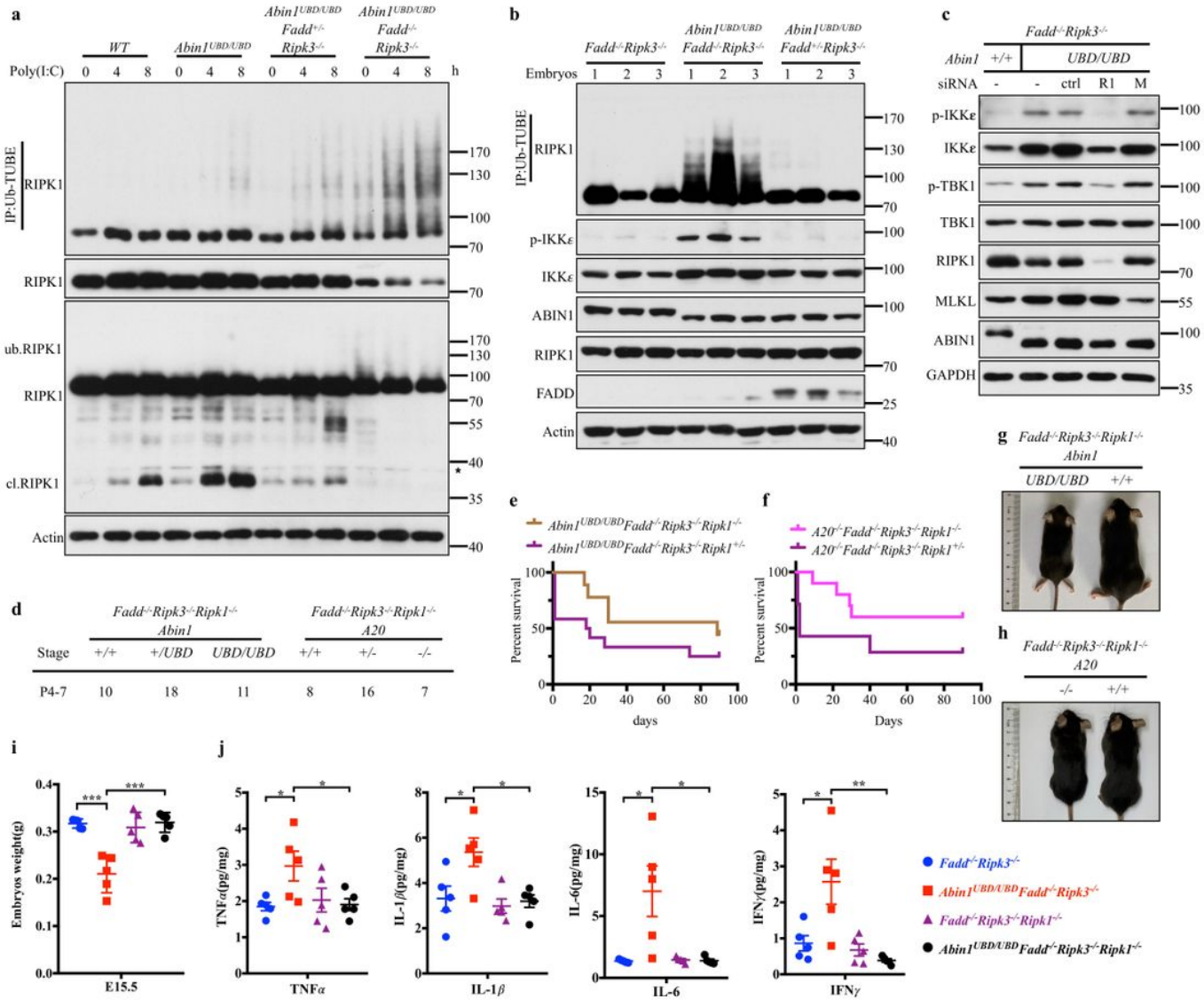

Figure 6

Knockout of Ripk1 rescue Abin1UBD/UBDFadd-/-Ripk3-/- and A20-/-Fadd-/-Ripk3-/- mice from embryonic or perinatal lethality, respectively. a. Immortalized MEFs were transfected with poly(I:C) for the indicated time, and cleaved and ubiquitylated RIPK1 were analyzed by western blotting. * indicated non-specific bands. b. Western blot of embryos at E14.5. High-molecular-weight ubiquitylated RIPK1 was pulled down by Ub-TUBEs and probed with an anti-RIPK1 antibody. c. Western blot of primary MEFs and Abin1UBD/UBDFadd-/-Ripk3-/- MEFs transfected with siRNAs targeting RIPK1 (R1), MLKL (M), or control (ctrl) for 48 h. d. Offspring numbers from intercrossing Abin1UBD/+Fadd-/-Ripk3-/-Ripk1-/- mice or A20+/-Fadd-/-Ripk3-/-Ripk1-/- mice, respectively. e-f. Survival curves of mice. Abin1UBD/UBDFadd-/-Ripk3-/-Ripk1-/- and Abin1UBD/ UBDFadd+/-Ripk3-/-Ripk1-/- mice (e). A20-/-Fadd-/-Ripk3-/-Ripk1-/- and A20-/-Fadd+/-Ripk3-/-Ripk1-/- mice (f). g-h. Representative macroscopic images of the eight-week-old littermates. i. Measurement of cytokines in the embryo homogenate at E15.5, with the indicated genotypes (n=5 embryos per genotype). j. Embryo weight at E15.5, with the genotypes indicated. Data represent mean± SEM; P values were determined using two-tailed Student's t-test, * $P<0.05$, ** $P< 0.01$, *** $P<0.001$.

Supplementary Files

This is a list of supplementary files associated with this preprint. Click to download.

- SupplementalFigures.pdf